Correcting Color-Measurement Error Caused by Stray Light in Image Scanners

Peter A. Jansson
DuPont Company, Wilmington, Delaware 19880-0357
and
Robert P. Breault
Breault Research Organization, Tucson, Arizona 85715

Abstract

All optical systems suffer from stray light due to undesired reflections plus light scattering from surface imperfections, dust, other particles and similar causes. This unwanted light flux can cause serious errors in imaging colorimetry and densitometry. Although minimizing stray-light error has heretofore required complex and expensive optomechanical scanner designs, simpler designs are sometimes preferred because of cost, or for remote detection applications. In this paper, we show that a color error of $\Delta E_{L^*a^*b^*} = 10$ or more is to be expected due to stray light alone in a simple imaging colorimeter, and that this error may easily be corrected† with inexpensive signal processing technology. Line scanners, densitometers, imaging radiometers, and on-line web-product inspection scanners can also benefit substantially.

Introduction

Controlling stray light has always been important in optical design.[1] Caused by phenomena such as Fresnel reflection from lens surfaces, air bubbles in glass, dust, diffraction at aperture edges, and numerous other effects, its presence frequently degrades both image contrast and measurement accuracy. Methods for control have included stops, baffles, apertures, black paint, and dielectric anti-reflection coatings for lenses. In single-color area-sensing colorimetry where sample contact is permitted, many of these means have been employed. Especially relevant in this application, however, is physical isolation of the desired sampling region so that all the light flux returned to the detector meets the geometrical definition required by the measurement. By this means, unwanted flux is excluded. Nevertheless, when the sensing region is nearly the same size as the illuminated region, lateral-diffusion error due to scattering can be problematic.[2]

When a large number of color measurements are required in sequence, as in image scanning, control of unwanted flux is challenging. The best stray-light reduction in image scanners is achieved by expensive, slow, and typically large high-end flatbed microdensitometers that employ mechanical reciprocating motion on both image Cartesian-coordinate axes. These units use a field aperture to define illumination for a single object or sample pixel, then image the reflected or transmitted flux into the plane of a receiving aperture, and finally detect the flux passing through this aperture. Although this technique has been known and applied to planar samples for years, it may now be best known for its modern use with volume samples in scanning confocal microscopy.

If the sample object is flexible, such as a photographic transparency, a rotary motion can replace the awkward high-speed reciprocating motion. Drum scanners based on this idea translate the aligned confocal illuminating and detecting modules along the axis of a rotating drum, about whose surface the transparency is wrapped. Although much faster than a two-axis flatbed, these units remain large, expensive, and too slow for many applications.

Convenient desktop scanning is now provided in flatbed units that have only one Cartesian axis of motion. These units typically illuminate a full line of pixels simultaneously and detect their fluxes simultaneously with a linear photodetector array. In these units, stray-light performance is compromised to achieve improved size, cost and speed. Each photodetector pixel element receives flux, not only from its desired conjugate pixel on the sample, but from neighboring pixels as well. The culprit is stray light due to scattering and undesired reflections.

Today, with the advent of continually improved area-sensing color scanners such as solid-state video cameras, researchers are beginning to apply this most-convenient no-moving-parts technology to color measurement.[3,4,5] Here, potential exists to spatially resolve and colorimetrically characterize multicolored samples and passively observed remote scenes. Even more than the single-line-illuminated flatbed, however, these imaging colorimeters are subject to errors caused by stray flux originating from sample locations outside the zone of interest. In the sections that follow we will show how severe the problem can be, and demonstrate that it can be corrected easily by a digital signal processor (DSP) working in real time. The problem to be solved is a close relative of the classic, often-ill-posed, inverse problem called deconvolution. *In the stray-light case, however, the nature of the spread function lends itself to robust and stable inversion when paired with a classic iteration scheme and a particular normalization.* Results can be applied to line-scan flatbeds, area-sensing imaging colorimeters, and many other types of densitometers and colorimeters.

Magnitude of the Error

For illustration purposes, we will choose an example from area-sensing imaging colorimetry. Prior work had given one of us experience imaging black and white transparency material back-illuminated with a diffusing light box and video camera.[6] In this application, opaque spots populated an essentially transparent background. The largest such spot extended over about 12 per cent of the image linear dimension, so that the spot covered approximately 1.44 per cent of the image area. The center of the opaque spot suffered stray-light contamination of about 2 per cent, thereby limiting the maximum optical density to a value of $D = \log(1.0/0.02) \approx 1.7$. The optical-density error was substantial; the result should have been infinite or undefined. Obviously readings close to $D = 1.7$ were meaningless and conveyed little or no information about the true transparency density. Even at lesser optical density, the same amount of stray light contributed serious error. For example, a pixel having a true optical density of 1.3 would give a reading of

$$D = \log_{10}\left(\frac{I_0}{I_d + I_s}\right) \approx 1.154, \qquad (1)$$

where the I_d is the direct flux having a value of $10^{-1.3} \times I_0 = .0501 \times I_0$ and I_s is the stray flux having a value of $0.02 \times I_0$. The error in optical-density units is therefore –0.146, or 11.2 per cent of the measurement. The density error described in the foregoing, which occurred at the center of a large spot, resulted from stray contributions associated with pixels quite distant from the affected pixel. Smaller spots, as well as densities measured in the same spot near its edge, suffered far greater error than this because stray-light contributions typically increase with decreasing distance between detection pixel and the detector-plane pixel conjugate to the source pixel. Knowing that stray light can have this disastrous impact on a densitometer, we were motivated to investigate its effect on color images.

Consider a color image acquired passively from a real-world scene by a solid-state video camera. By analogy with the densitometer example cited above, comparable levels of stray light should contaminate image spots having comparable area. In particular, consider the example of imaging a blue flower on a green grass field. Assume the green field has CIE color coordinates of 10, 30, and 10, respectively, in the XYZ system.[7] Likewise give the blue flower coordinates of 10, 10, 30. Because the XYZ system is radiometrically linear, we readily obtain the coordinates of the contaminated blue color by adding 5 per cent of the green flux to 95 per cent of the blue flux. See Fig. 1. The result is an XYZ measurement of 10, 11, and 29. To place this result in perceptual perspective, convert the three sets of coordinates to the L*a*b* space, which is perceptually uniform to good approximation. The color difference between measured and true values for blue are given by the Euclidean distance between the two colors in this space as $\Delta E_{L^*a^*b^*} = 8.94$. We illustrate this computation in Fig. 1.

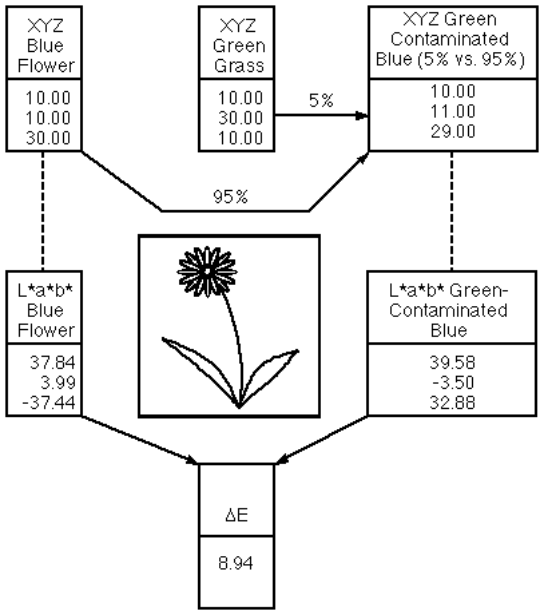

Figure 1. Error introduced by stray light contaminating the image of a blue flower on a green field

Analogous computation for a more saturated green (6.5, 40, and 2.5) and blue (6.5, 2.5, and 40) with only 2 per cent contamination gave $\Delta E_{L^*a^*b^*} = 15.07$. Contamination of 4% white background in a 5% reflecting or transmitting black spot gave a $\Delta E_{L^*a^*b^*} = 9.09$.

Again, our computation is conservative because we considered measurements at the center of a large spot. Because stray light originating from a given pixel most severely affects its closest neighbors, we expect color error for small-spot measurements to be much larger. To accurately gauge the magnitude of this error in practice, and to allow for its correction, we need to characterize and quantitate the phenomena contributing to the stray light.

Stray-Light Function and Its Characterization

Optical systems can be characterized by the way in which they collect multi-angle flux originating from a single point on an object and concentrate it in the image plane. Ideally, in the geometrical optics approximation, the image-plane flux corresponding to a single object point ought to be itself a single point. Real optical systems, however, are subject to geometrical aberrations, diffraction, and in the present discussion, stray light. Flux originating from a single object point is therefore spread over a finite region in the image plane. The function characteristic of this spread is called the point-spread function or PSF. Typical analyses neglect stray light and consider the relatively small-cored PSF that results from diffraction and aberrations. Here we consider a PSF that includes stray flux originating from any point in the image and being received at any other point. The stray-flux part of the PSF may vary slowly, but could

also contain contributions from sharper structure such as ghost images and specular glints.

For simplicity in the following discussion, let us consider, without loss of generality, a line scanner in which only one spatial axis requires consideration. (The finite-extent two-dimensional case can also readily be formulated with one independent variable.[8]) Let $s(x,x')$ be the PSF of such a scanner in which the flux received by a detector having coordinate x along an image line is given by

$$i(x) = \int s(x,x')o(x')dx', \tag{2}$$

where $o(x')$ is the flux emanating from points along some object line having coordinate x'. The limits of the integral are taken to cover the entire object. A PSF requiring a single independent variable is said to be shift-invariant. The scanner it describes can be termed isoplanatic. In this case, the spreading characteristic relative to neighboring image points is independent of spatial location. More realistic is the shift-variant case in which two independent variables are required. For a scanner with a shift-invariant PSF, Eq. (2) becomes a convolution.

A number of optical phenomena affecting the form of $s(x,x')$ vary with the wavelength of light. Among these are the scattering of light by dust particles, bubbles and surfaces, wavelength dispersion of light by dielectrics, and diffraction. We may understand Eq. (2) to be valid at just one wavelength, or we may include wavelength as a variable λ, thereby giving

$$i(x,\lambda) = \int s(x,x',\lambda)o(x',\lambda)dx'. \tag{3}$$

However, consider also that, for color-measurement purposes, we compute tristimulus values from equations[7] having the form $Y = \int \bar{y}(\lambda)I(\lambda)d\lambda$, where Y is one of the three tristimulus values X, Y, and Z representing the eye's response to a polychromatic chromatic flux $I(\lambda)$ incident upon it, and $\bar{y}(\lambda)$ is the CIE standard-observer luminosity function. The quantities X and Z are computed from like equations in which $\bar{y}$ is substituted by the other two standard-observer functions $\bar{x}$ and $\bar{z}$, respectively.[7] From these definitions, we may see that the eye's response to a spatially varying flux $i(x,\lambda)$ is typified by

$$Y_i(x) = \int \bar{y}(\lambda)i(x,\lambda)d\lambda. \tag{4}$$

Substituting Eq. (3) into Eq. (4), we find that

$$Y_i(x) = \int \bar{y}(\lambda)\left[\int s(x,x',\lambda)o(x',\lambda)dx'\right]d\lambda. \tag{5}$$

Reversing integration order, we note that the PSF may be removed from the integrand only if it is wavelength-independent. In this case we obtain

$$Y_i(x) = \int s(x,x')\left[\int \bar{y}(\lambda)o(x',\lambda)d\lambda\right]dx'. \tag{6}$$

Therefore the equivalent visual Y-response to polychromatic flux $o(x',\lambda)$ that has passed through the scanner is perfectly well modeled by applying the imaging equation to the spatially varying tristimulus-integrated object flux $o(x',\lambda)$, so that

$$Y_i(x) = \int s(x,x')Y_o(x')dx', \tag{7}$$

where $Y_o(x) = \int \bar{y}(\lambda)o(x',\lambda)d\lambda$. Analogous equations obtain for the X and Z values. Thus we see that Eq. (2), the imaging equation, is equally applicable to spatially varying tristimulus values as it is to monochromatic fluxes but rigorously only for the case in which the PSF is wavelength-independent. Nevertheless, wavelength independence may be a useful approximation for practical applications. With these caveats in mind, for simplicity of notation we suppress the wavelength dependence of variables in the balance of this paper.

Removing the stray-light contribution from the image data $i(x)$ requires specific knowledge of the PSF $s(x, x')$ that affected those data. The definition of $s(x, x')$ suggests its most direct means of determination. One can introduce a small light source, approximating a point, into the object plane, then measure detector responses in the image plane. Alternately, one could measure a known test object such as one approximating a Heaviside step,[9] and then use these data to compute the PSF.

Correcting the Image

A classic method of solving Eq. (2) for $o(x)$, where $s(x, x')$ is a convolution kernel, has been in use since Van Cittert[10] first applied it to X-ray data in 1931. His method[8] generates a succession of improved object estimates

$$\hat{o}^{(k+1)} = \hat{o}^{(k)} + (i - s \otimes \hat{o}^{(k)}), \tag{8}$$

given a starting-point estimate $\hat{o}^{(0)}$. Here we have suppressed the variable dependence for clarity and used the operator "$\otimes$" to denote convolution. Van Cittert's method, when it converges, converges to a simple inverse filter.[8] It is a linear deconvolution method and is normally subject to all the attendant difficulties of linear methods applied to ill-posed deconvolution problems.[8] In the following section, we will demonstrate that *correcting images for stray-light contamination is not ill-posed*, and is therefore responsive to the method. For the purpose of further discussion, we will generalize the Van Cittert method to the shift variant case, which is realistic for the stray-light problem, and let the "$\otimes$" operator denote the integral operation for both cases. The discrete-sampled Van Cittert method for this case is identical to the Jacobi method for iteratively solving a set linear equations.[8]

PSF Normalization and the First Object Estimate

We tailor Van Cittert's method to the stray-light case by accounting for specific features of the stray-light PSF $s(x, x')$. In particular, let $s_p(x, x') = \delta(x - x')$, the Dirac delta function, denote the PSF of an idealized "perfect" scanner not subject to image contamination by stray light, and $s_D(x,x')$ describe purely the stray-light component, so that we have

$$s(x) = s_p(x) + s_D(x) \tag{9}$$

for a real scanner. Note that because $\int \delta(x)dx = 1$, we have tacitly assumed that the integral of the "perfect" part of s is normalized to unity so that necessarily

$$\int s_p(x,x')dx' = \int s_p(x',x)dx' = 1 \tag{10}$$

for all x, and

$$\int s(x,x')dx' = \int s(x',x)dx' > 1 \tag{11}$$

for all x. This normalization is relevant and in fact essential, not necessarily in general but to facilitate the result that follows immediately.

In using Van Cittert's method, one typically assumes an initial object estimate $\hat{o}^{(0)} = i$. Applying that assumption in the present case, we obtain by substitution

$$\begin{aligned}\hat{o}^{(1)} &= (i) + (i - s \otimes i) \\ &= (s_P \otimes o + s_D \otimes o) + [(s_P \otimes o + s_D \otimes o) \\ &\quad - s_P \otimes s_P \otimes o - 2s_P \otimes s_D \otimes o - s_D \otimes s_D \otimes o].\end{aligned} \tag{12}$$

Noting the normalization of s_P and collecting terms, we find

$$\hat{o}^{(1)} = o - s_D \otimes s_D \otimes o. \tag{13}$$

This is an especially interesting result, a serendipitous consequence of the choice for normalizing the PSF. We have found that the first iteration object estimate is indeed the object itself, in error by only the term $-s_D \otimes s_D \otimes o$, which is relatively small because

$$\int s_D(x,x')dx' << \int s_P(x,x')dx' \tag{14}$$

for all x for most scanners in practice! Let us see how well it works.

Results with Simulated Data

To test the algorithm's capability to remove stray-light contamination, we synthesized a monochromatic one-dimensional object having six spots, each having a Gaussian flux profile. See Fig. 2. The spots each had a half-width at half maximum (HWHM) of $10/\sqrt{\ln 2}$ pixels. They had amplitudes of 0.3, 0.6, 0.8, 0.1, 0.2, and 0.5, and were located in a 1000 pixel image at pixel locations 253, 500, 540, 605, 635, and 640, respectively. We numerically approximated a scanner PSF that superposed a delta-function core (written here as a narrow gaussian) on a stray-light "skirt" that fell off inversely with distance at large distance from the core:

$$\begin{aligned}s(x) &= s_P(x) + s_D(x) \\ &= \left[exp\left[-(1000x)^2\right] + \frac{1}{100(|x|+1)} \right] \Big/ 1.01.\end{aligned} \tag{15}$$

The quantity 1.01 in the denominator of Eq. (15) provided normalization in a manner consistent with foregoing Eq. (10). We used discrete circular convolution to contaminate the synthetic object in a manner analogous to Eq. (2), the imaging equation, and display the result in Fig. 3.

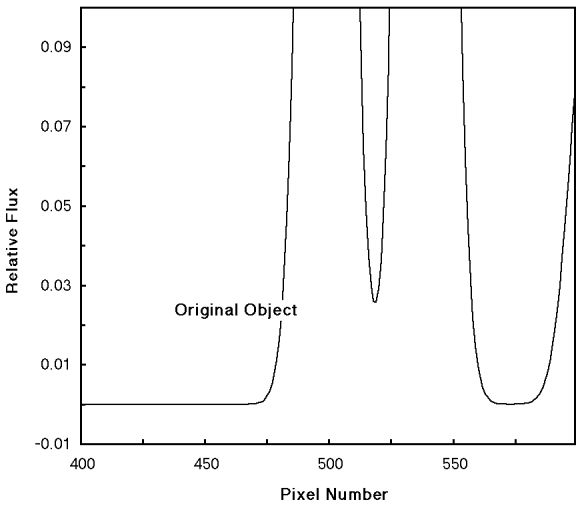

Figure 2. Portion of one-dimensional object

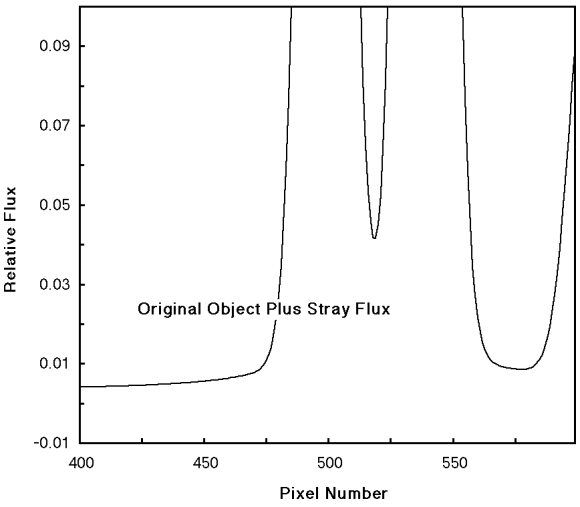

Figure 3. Object contaminated by stray light flux

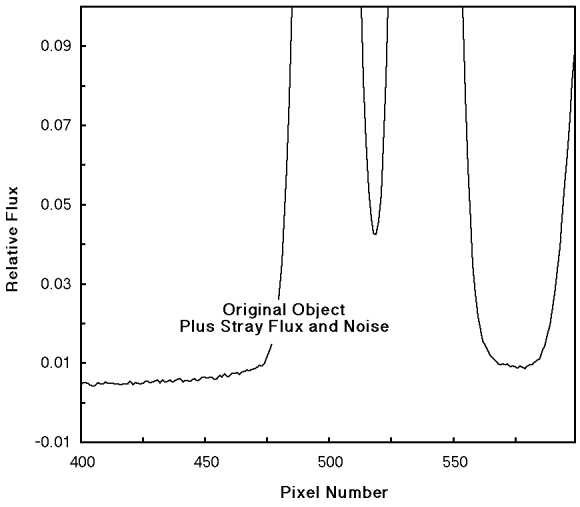

Figure 4. Object contaminated by stray light and detection noise

Virtually perfect deconvolution is possible even with the most difficult PSF's when data are essentially noise-free. To provide a fair test of the method, we added random noise uniformly distributed over the interval from 0 to 0.001 (see Fig. 4).

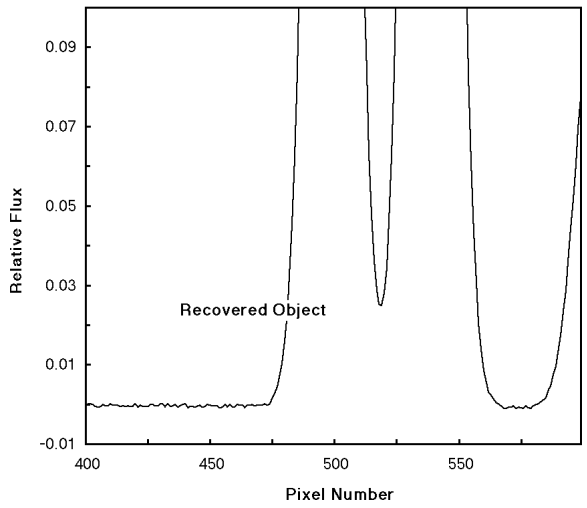

Figure 5. Restored object; Image corrected by removing stray-light contribution

The result of the stray-light correction appears in Fig. 5. This figure shows an ordinate-magnified portion of first object estimate $\hat{o}^{(1)}$. In this figure, we see that the stray-light contribution is reduced by *well over an order of magnitude*. Furthermore, the original object is reproduced with excellent fidelity. A comparable reduction in a densitometer's stray light corresponds to more than one full optical-density unit improvement in a densitometer's useful range. In an imaging colorimeter, this performance-limiting error is virtually eliminated. By this, we mean that the stray-light-induced color error can be reduced below the level resulting from other error sources. United States[11] and foreign patents have been awarded for this improvement to image scanning.

Conclusion

We have demonstrated the correction of color error induced by light stray-light levels typical of those found in modern high-speed densitometers and imaging colorimeters. The correction method has the potential to eliminate this error as a serious limitation of these instruments. We achieved our objective by adapting a classic linear deconvolution method to the more general task of removing shift-variant stray-light contamination from the scanned images. Operating directly in signal space, one cycle of correction was sufficient. A particular PSF normalization was key to achieving the objective of extremely rapid convergence. Additional cycles could readily be added but are probably not required. With suitable attention to data-sampling issues and code efficiency, an embedded DSP could perform the correction in real time, and in a manner transparent to the user. Our technology is believed to have commercial potential in scanning densitometers, area-sensing and line-scanning imaging colorimeters, imaging radiometers, and for on-line inspection of web products such as multicolored textiles and printed matter.

Acknowledgments

The authors are grateful to P.M. Tannenbaum and R.W. Gruhlke for reading the manuscript and for helpful criticism. They also wish to thank D.L. Spooner for valuable discussions.

References

† U. S. Patent #5,153,926

1. R. P. Breault, "Control of Stray Light" in *Handbook of Optics*, Vol. I, McGraw-Hill, Inc., New York, 1995, pp. 38.1-38.35.
2. D. L. Spooner, *TAGA Proceedings*, pp. 130-143 (1991).
3. M. L. Simpson and J. F. Jansen, *Applied Optics* **30**, 4666-71 (1991).
4. J. R. Dymond and C. M. Trotter, *Applied Optics* **36**, 4314-8 (1997).
5. I. Réti and I. Giczi, *Optical Engineering* **32**, 2578-80 (1993).
6. P. A. Jansson, L. B. Grim, J. G. Elias, E. A. Bagley, and K. K. Lonberg-Holm, *Electrophoresis* **4**, 82-91 (1983).
7. D. B. Judd and G.Wyszecki, *Color in Business, Science, and Industry*, 3rd ed., J.Wiley and Sons, New York, 1975.
8. P. A. Jansson, ed., *Deconvolution of Images and Spectra*. Academic Press, New York, 1996, pp. 84-5.
9. P. A. Jansson, ed., *Deconvolution of Images and Spectra*. Academic Press, New York, 1996.
10. P. H. van Cittert, *Z. Phys.* **69**, 298-308.
11. P. A. Jansson and J. H. Fralinger, "Parallel processing network that corrects for light scattering in image scanners," U. S. Patent #5,153,926.